Letter

Chinese Science Bulletin

Condensed Matter Physics

January 2012 Vol.57 No.1: 68–71
doi: 10.1007/s11434-011-4810-7

Thermal detection of surface plasmons on gold nanohole arrays

ZHANG Wei[1], LI ZhiPeng[2], GUAN ZhiQiang[1], SHEN Hao[1], YU WenBo[3], He WeiDong[3], YAN XiaoPeng[3], LI Ping[3] & XU HongXing[1,4*]

[1] *Beijing National Laboratory for Condensed Matter Physics, Institute of Physics, Chinese Academy of Sciences, Beijing 100190, China;*
[2] *Beijing Key Laboratory of Nano-Photonics and Nano-Structure (NPNS), Department of Physics, Capital Normal University, Beijing 100048, China;*
[3] *Information Awareness and Confrontation, Beijing Institute of Technology, Beijing 100081, China;*
[4] *Division of Solid State Physics, Lund University, Lund 22100, Sweden*

Received May 5, 2011; accepted July 1, 2011

We used a thin-film thermocouple to detect the thermal effect of surface plasmons excited in Au nanohole array structures. We found that the thermal electromotive force of Au film with periodic nanohole structures is three times greater than that of a bare Au film for 785-nm laser excitation at a given power. This effect is caused by the resonant excitation of localized surface plasmons in the nanoholes. In addition, we found that the thermal electromotive force (EMF) of the Au film with dumbbell-like nanohole arrays depends strongly on the incident polarization. The thermal EMF is the greatest when the excitation light is polarized perpendicular to the long axis of the dumbbell.

surface plasmons, thermal effect, thin film thermocouple, periodic structure

Citation: Zhang W, Li Z P, Guan Z Q, et al. Thermal detection of surface plasmons on gold nanohole arrays. Chin Sci Bull, 2012, 57: 68–71, doi: 10.1007/s11434-011-4810-7

Recently, the thermal properties of surface plasmons (SPs) have gained increasing attention because of their potential applications in various fields. For instance, the use of Au nanoparticles as nanosources of heat already have had promising applications in nanoscale catalysis [1], magnetism [2], microfluidics [3,4], phononics [5,6], and medicine, such as photothermal cancer therapy [7] or drug delivery [8]. Boyer et al. used the polarization interference method to obtain an image of nanometer-sized metal particles, based on slight phase changes induced by the heating of metal particles [9]. Quidant et al. used a method based on fluorescence polarization anisotropy to detect the thermal effect in Au nanoparticles [10]. Metal thin films with periodic nanoholes have very strong tunable SP resonances that range from visible to infrared, which can be adjusted by tuning the size of nanoholes, the inter-hole distance, and the thickness of the film [11–13]. Thin-film thermocouples provide a sensitive way to make accurate and fast surface temperature measurements (as low as ~1 μs response time), which provides many advantages: close thermal contact with the surface, low thermal inertia (mass ~10^{-4} g), high spatial resolution, and low cost [14]. By modifying thin-film thermocouples with plasmonic nanohole structures on one of the electrodes, very sensitive thermoelectric detection of SPs can be achieved.

In this study, we investigated the thermal effect of SPs excited on Au thin film with periodic nanohole structures using thin-film thermocouples. An electrode made from a Au thin film was fabricated on an electrode of Ni film to form a thin-film thermocouple. SPs on the Au nanostructures were excited by incident lasers with different wavelengths. The decay of SPs via Ohmic loss resulted in heat transfer. The temperature difference between the Au film and the Ni film produced a thermal electromotive force (EMF) when the incident light excited the SPs of the Au film. With this method, the thermal effect of SPs, which is proportional to the intensity of the incident light, can be measured.

*Corresponding author (email: hxxu@aphy.iphy.ac.cn)

The samples were fabricated via the pattern-overlay method with a Raith150 system (Raith Company, Germany). A schematic of the device is shown in Figure 1(a). First, a layer of 250-nm-thick polymethyl methacrylate (PMMA) electron-sensitive resist was spin-coated onto the Si substrate, which is insulated by a layer of 300-nm-thick SiO_2, and was pre-baked at 180°C for 60 s on a hotplate. Then, the pattern for the Ni electrode was exposed at a voltage of 20 kV and a dose of 120 μC/cm^2 via electron beam lithography (EBL). The pattern was generated in the PMMA layer after development in a 1:3 methyl isobutyl ketone/isopropanol (MIBK/IPA) PMMA developer for 60 s. It was then rinsed with IPA for 30 s and blow-dried with pure nitrogen gas. A 100-nm-thick Ni film was then evaporated onto the surface via our thermal evaporation system. The samples were immersed in acetone for 12 h to remove the PMMA layer and rinsed with deionized water, completing the fabrication of the Ni electrode layer. We used the same method to fabricate Au thin films with or without nanohole arrays on top of the Ni layer. The patterns for the Au film electrodes with or without a nanohole arrays were made using an EBL system. A 100-nm Au film was then evaporated onto the pattern, and the remaining PMMA layer was removed. This process was used for Au film electrodes with or without nanohole arrays.

To measure the thermoelectric effect of the thin-film thermocouple obtained in the manner described above, the area on the Au film with the nanohole array was excited using an ~2-μm laser spot at the sample, which was achieved by passing the beam through a 50× (NA = 0.50) objective. This is shown in Figure 1(b). The intensity of the laser can be adjusted using the attenuator, and the polarization of the incident laser can be adjusted using the half-wave plate. The thermal EMF was detected via a Thurlby-1905a digital multimeter (Thurlby Thandar Instruments, United Kingdom).

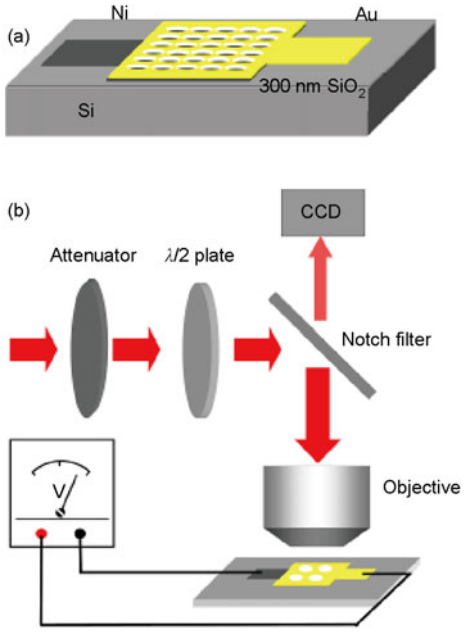

Figure 1 (a) Schematic drawing of the device; (b) schematic drawing of the experimental setup. A Thurley-1905a multimeter was used to detect the thermal EMF of the sample.

Figure 2(a) shows a scanning electron microscope (SEM, Goindustry Dovebid, America) image of the sample with a nanohole array on the thin Au film. Figure 2(b) shows the sample without nanohole structures. The average diameter of the holes in Figure 2(a) is 380 nm and the lattice separation is 500 nm. All the patterns in Figure 2(a) and (b) have an area of 20 μm×20 μm. According to previous research [12], the plasmon resonant peak for such Au nanohole structures is at ~785 nm. We used a 785-nm laser to excite the SPs of these structures. Figure 2(c) shows the thermal EMF for these structures versus the intensity of the incident laser. The black squares are the experimental data for the Au film with a nanohole array, and the grey dots are the data for the bare Au film. As the incident power of the 785-nm laser increases, the thermal EMF for the Au film with the nanohole array increases much faster than that for the Au film without nanoholes. In the inset of Figure 2(b), we show that the Au film prepared by vapor deposition is very rough. The roughness of the surface favors the coupling of the incident light to SPs in the Au film and increases the absorption of light by the Au nanoprotrusions at the surface of the Au film. The temperature of the bare Au film can thus still increase with an increase of the incident laser power. However, the thermal EMF for the Au film with nanohole array structures can be almost three times more intense than that for the bare Au film. This demonstrates that the periodic nanohole array can couple the incident light to SPs more efficiently than the rough surface, and will result in higher sensitivity for the thermoelectric detection of the incident light.

As shown in Figure 2(c), the thermal EMF increased nearly linearly as the intensity of the incident laser increased. This can be fitted using $\Delta U = \beta \cdot I = \alpha \cdot \Delta T$, where ΔU is the thermal EMF of the thermocouple; β is the fitting coefficient; I is the incident power; α is the thermoelectric coefficient (~20 μV/K for an Au-Ni thin-film thermocouple [14]); and ΔT is the temperature difference in the thin-film thermocouple. The thermal EMF at an incident laser power of 8 mW can reach values greater than 600 μV, which correspond to a temperature difference of more than 30 K between the Au film with nanohole arrays and the Ni film. Hence, SPs excited on Au nanohole array structures can be detected thermoelectrically.

For the sample in Figure 2, we also used non-resonant laser wavelengths of 514 and 633 nm to excite these structures. We found that the thermal EMF produced when the sample was excited by these wavelengths was much less than that when the sample was excited at 785 nm. In addition, when excited by 514-nm and 633-nm lasers, the difference in the thermal EMF between periodic sub-wave-

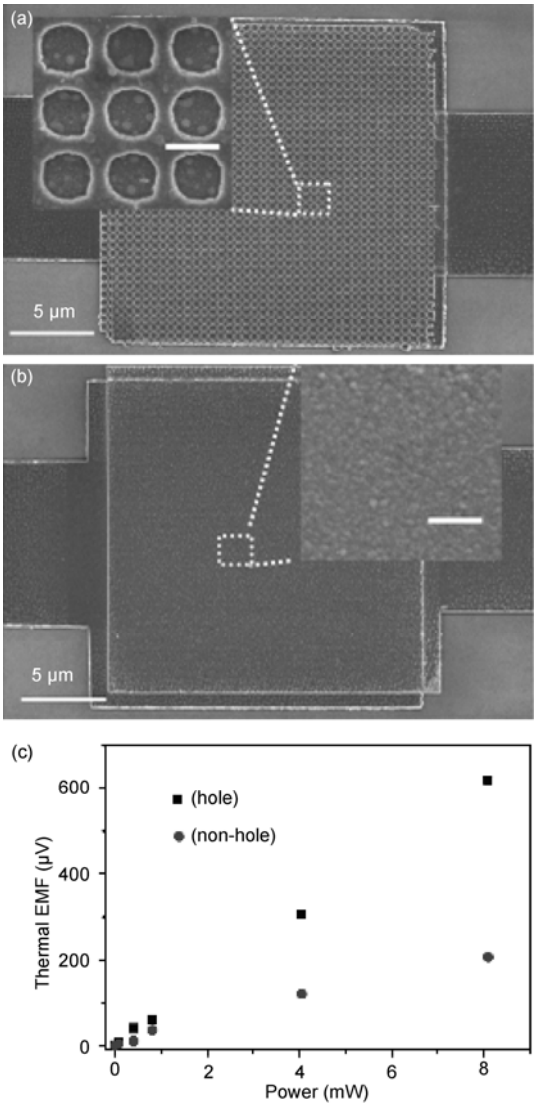

Figure 2 (a) SEM image of a Au film with a Au nanohole array. The average diameter of the hole is 380 nm and the lattice separation is 500 nm. (b) SEM image of the contrast sample with nanoholes. The scale bars in the insets of (a) and (b) are 500 nm. The thicknesses of the Au and Ni films are both 100 nm. (c) The thermal EMF of the sample with nanoholes (black squares) and without nanoholes (grey dots). The excitation laser is 785 nm, and the incident polarization is kept parallel during laser illumination.

length holes and non-hole structures was small. Therefore, we believe that the significant thermal effect for the nanohole arrays excited by a 785-nm laser results from the resonant surface plasmon excitation. When the excitation light is incident on the nanohole array, both localized and propagating SPs can be excited in this structure [15–17]. However, the electromagnetic energy is mainly concentrated around the nanoholes when these structures are excited with a resonant wavelength [18,19]. Thus, we speculate that the enhancement of the EMF to three times that of bare Au films is caused mainly by the localized SPs in the nanohole structures.

To further understand the thermoelectric detection of SPs, we used the fabrication method described above to make a dumbbell-like nanohole array on a thin Au film. This is shown in the inset of Figure 3. The average diameter of the nanohole is ~190 nm, and the center-to-center distance of the dumbbell is about 210 nm. The gap between the two protrusions in the middle of the dumbbell-like structure is less than 30 nm. Various laser wavelengths (514, 633 and 785 nm) were used to excite this structure. However, the signals were very weak when excited by the 514-nm and 785-nm laser light. When excited by the 633-nm laser, stronger signals were detected. Therefore, 633 nm is close to the SP resonance wavelength for this structure. Figure 3 shows the corresponding thermal EMF data for different polarizations of the 633-nm laser. When the laser was polarized parallel to the long axis of the dumbbell ($\theta = 0$), the thermal EMF was weakest, but when the laser was polarized perpendicularly to the long axis ($\theta = 90$), the thermal voltage reached its maximum. This is because the electromagnetic field intensity in the gap between the two protrusions strongly depends on the incident polarization. In this structure, the gap between the two protrusions is the "hot spot" and contributes mainly to the stronger thermal EMF for the polarization perpendicular to the long axis of the dumbbell. The strong electromagnetic field intensity in the gap is caused by both the lightning-rod effect [20] and the plasmon coupling of the two protrusions [21,22]. When the incident polarization is perpendicular to the long axis of the dumbbell, the local electromagnetic field in the gap can be enhanced dramatically, which results in the strong EMF signal.

From the data shown above, we showed that the thin-film thermocouple can effectively detect the thermal effect of surface plasmons and thus realize the detection of the light.

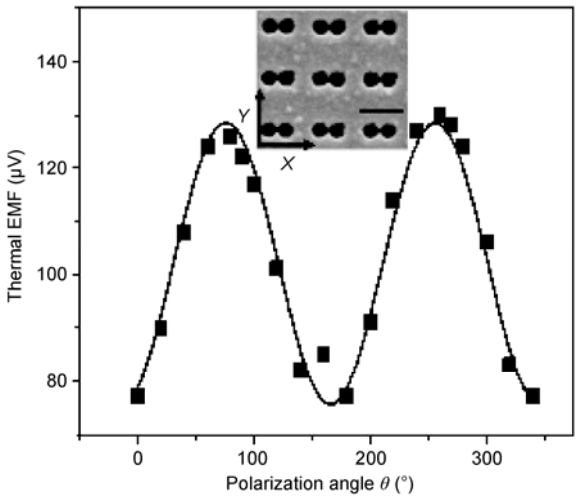

Figure 3 The thermal effect of the Au film with a dumbbell-like nanohole array versus the incident polarization angle θ, which is the angle between the x axis and the incident polarization. The inset shows an SEM image of a Au dumbbell-like nanohole array with an average hole diameter of 190 nm, a center-center distance of the dumbbell of 210 nm, and a lattice separation of 600 nm. The scale bar in the inset is 500 nm. The thickness of the Au/Ni films is both 100 nm. The excitation laser wavelength is 633 nm and the incident power is 5.8 mW. The polarization of the incident light can be adjusted via the half-wave plate.

The resonance frequency of surface plasmons can be tuned over the range from visible to infrared light by tuning the parameters of periodic structures, such as the diameter, shape, and orientation of the holes; the periodicity of the array; the film thickness; and the film material [15]. Through careful design of the nanostructure, it is possible to alter the SP resonance frequency. It is also possible to develop a new type of infrared detector [13] to fill the detection gap in the mid-infrared spectral range.

In summary, we used the thin-film thermocouple to detect the thermal effect from surface plasmons excited in Au nanohole array nanostructures. We found that the thermal electromotive force for Au film with periodic nanohole structures can be three times greater than that for bare Au film under the same power of 785-nm laser excitation. This is mainly caused by the resonant localized surface plasmons in the nanoholes. In addition, we investigated the thermal effect of Au film with a dumbbell-like nanohole array, and found that the thermal electromotive force became highly dependent on the incident polarization. When the excitation light was polarized perpendicular to the long axis of the dumbbell, the thermal EMF was the greatest.

This work was supported by National Natural Science Foundation of China (*10874233*)*, National Basic Research Program of China* (*2009CB930700*) *and Knowledge Innovation Project of Chinese Academy of Sciences* (*KJCX2-EW-W04*).

1 Cao L Y, Barsic D N, Guichard A R, et al. Nano Lett, 2007, 7: 3523–3527
2 Challener W A, Peng C B, Itagi A V, et al. Nat Photonics, 2009, 3: 220–224
3 Liu G L, Kim J, Lu Y, et al. Nat Mater, 2006, 5: 27–32
4 Miao X Y, Wilson B K, Lin L Y. Appl Phys Lett, 2008, 92: 124108
5 Wang L, Li B W. Phys Rev Lett, 2008, 101: 267203
6 Wang L, Li B. Phys Rev Lett, 2007, 99: 177208
7 Lal S, Clare S E, Halas N J. Acc Chem Res, 2008, 41: 1842–1851
8 Han G, Ghosh P, De M, et al. NanoBiotechnology, 2007, 3: 40–45
9 Boyer D, Tamarat P, Maali A, et al. Science, 2002, 297: 1160–1163
10 Baffou G, Girard C, Quidant R. Phys Rev Lett, 2010, 104: 136805
11 Ebbesen T W, Lezec H J, Ghaemi H F, et al. Nature, 1998, 391: 667–669
12 Yu Q M, Guan P, Qin D, et al. Nano Lett, 2008, 8: 1923–1928
13 Fang X, Li Z Y, Long Y B, et al. Phys Rev Lett, 2007, 99: 066805
14 Thornburg D D, Wayman C M. J Appl Phys, 1969, 40: 3007–3013
15 Genet C, Ebbesen T W. Nature, 2007, 445: 39–46
16 Bao Y J, Peng R W, Shu D J, et al. Phys Rev Lett, 2008, 101: 087401
17 Gao H W, Henzie J, Odom T W. Nano Lett, 2006, 6: 2104–2108
18 Salomon L, Grillot F, Zayats A V, et al. Phys Rev Lett, 2001, 86: 1110–1113
19 Wei H, Hakanson U, Yang Z L, et al. Small, 2008, 4: 1296–1300
20 Gersten J, Nitzan A. J Chem Phys, 1980, 73: 3023–3037
21 Xu H X, Bjerneld E J, Kall M, et al. Phys Rev Lett, 1999, 83: 4357–4360
22 Xu H X, Aizpurua J, Kall M. Phys Rev E, 2000, 62: 4318–4324